Functional Materials 18, No.3 (2011)

An influence of transition metal ions impurities on the luminescence of $Li_2Zn_2(MoO_4)_3$ crystals

V.A.Nadolinny, A.A.Pavluk, A.A.Ryadun, A.A.Trifonov, C.F.Solodovnikov, Z.A.Solodovnikova, E.S.Zolotova, V.F.Plyusnin*, M.I.Rakhmanova, E.G.Boguslavsky

A.Nikolaev Institute of Inorganic Chemistry, Siberian Branch of Russian Academy of Sciences, 3 Acad. Lavrentiev Ave., 630090 Novosibirsk, Russia

*Institute of Chemical Kinetics and Combustion, Siberian Branch of Russian Academy of Sciences, 3 Institutskaya Str., 630090 Novosibirsk, Russia

Received February 2, 2011

The optimal conditions for $Li_2Zn_2(MoO_4)_3$ crystal growth were selected on the basis of corrected phase diagram. Large undoped and activated by transition metal ions (Cu, Cr, Fe, Ti) crystals were grown upon these conditions. Charge state and structural position of transition metal ions were determined by EPR method. Investigations of luminescence shown that the luminescence with λ = 388 nm is observed for undoped crystals at room temperature. The luminescence lifetime is described by two exponential components, with relaxation times τ_1 = 2 ns and τ_2 = 6 ns. The luminescence with λ = 560 nm and lifetime τ = 100 nm is observed as for undoped, so as for activated by transition metal ions crystals at 77 K. Besides, the luminescence intensity with λ = 560 nm depends on nature and concentration of transition metal ions. It is supposed, that cation vacancies, which ensure the charge compensation of the impurity transition metal ions, are responsible for the low-temperature luminescence.

На основании откорректированной фазовой диаграммы выбраны правильные условия роста кристаллов $Li_2Zn_2(MoO_4)_3$ и выращены крупные кристаллы (до 100 мм) как беспримесные, так и активированные ионами переходных металлов - Cu, Cr, Fe, Ti. Методом ЭПР установлено зарядовое состояние и структурное положение ионов переходных металлов. Проведенные исследования люминесцентных свойств показали, что для беспримесных кристаллов при комнатной температуре наблюдается люминесценция с λ = 388 нм с двухэкспоненциальным спадом люминесценции с τ_1 = 2 нсек и τ_2 = 6 нсек. При 77 К как для беспримесных, так и для активированных ионами переходных металлов кристаллов наблюдается люминесценция с λ= 560 нм и временем жизни люминесценции τ = 100 нсек, причем интенсивность люминесценции с λ= 560 нм зависит от природы и концентрации ионов переходных металлов. Предполагается, что за низкотемпературную люминесценцию отвечают катионные вакансии, ответственные за зарядовую компенсацию примесных ионов переходных металлов.

1. Introduction

The wide use of scintillation crystals in medicine, nuclear research and space programmes stimulates and intensifies a competition between various crystals growth groups in the world in search for new scintillation materials with higher light output, light emission in a definite wavelength

range and shorter decay times. The basic requirements for scintillators by these spheres of practical application are the following: an increase in luminosity and decrease in decay time till 10 ns for enhancing energy resolution and reducing exposure doses under using in medical tomography machines [1]. In the 1990s the scintillating characteristics of cerium ion-activated Lu_2SiO_5 (LSO), $Lu_2Si_2O_7$ and $LuAlO_3$ crystals [2–6] have been revealed, that combine a large effective atomic number, high light output and a short decay time. The discovery of the new scintillation crystals — cerium-activated lanthanum halogenides ($LaBr_3$:Ce, $LaCl_3$:Ce) in 2000 aroused a great interest [7]. Having a light output comparable with that of NaI:Tl, they provide a considerably higher energy resolution (approx. 3 % at 662 keV) as well as a short decay time (approx. 15–25 ns). All the above mentioned scintillation materials did not widely use because of the complexity and expensiveness of growing large crystals.

Recently the interest of researchers has recently shifted to the field of hexavalent molybdenum oxide compounds, in particular due to the fact that these compounds provide a means of solving the problem of recording neutrinoless double beta decay ($0\nu2\beta$) [8]. The significant interest to this problem is connected with determination of neutrino mass, while ^{100}Mo is one of the most promising nuclei for 2β-decay experiments due to its high transition energy $Q_{2\beta} = 3035$ keV [9]. Thus, molybdates monocrystals can be potentially used as detectors in such experiments. Oxide crystals for cryogenic bolometric detectors of 2β-decay must have high light output and transparency, a short afterglow time, a high content of the element studied (here Mo) without any radioactive impurities, as well as be diamagnetic for attainment of low temperatures measurement. Low density and a small effective atomic number are also desirable for reducing the γ-background. However, tested crystals of simple molybdates $MMoO_4$ (M = Pb, Mg, Ca, Cd) [10–14] possess a number of disadvantageous features (presence of natural radioactive impurities, a high effective atomic number, low light output etc.), which stimulates search for new crystals with suitable composition and properties.

In recent years there have appeared publications on growing and studying properties of $ZnMoO_4$ crystals [15, 16] and $Li_2Zn_2(MoO_4)_3$ double molybdate crystals [17, 19]. The authors of the publications [17, 19] were only able to grow crystals using the Czochralski method with dimensions in centimetre range, which seems to be primarily connected with the problem of growth of large homogeneous $Li_2Zn_2(MoO_4)_3$ crystals. Another impeding problem could have been the possible nonstoichiometry of this compound, which prevents creating the optimal conditions for crystal growth and causes crystal inhomogeneity and formation of other phases. But this possibility has not been taken into account before in studying the phase diagram of the Li_2MoO_4–$ZnMoO_4$ system [19, 20].

In the present work on the basis of the results of our new study for the Li_2MoO_4–$ZnMoO_4$ system phase diagram [21] optically homogeneous and virtually stoichiometric $Li_2Zn_2(MoO_4)_3$ crystals, both pure and doped with different transition metal ions, have been grown by the low-gradient Czochralski method. We also have investigated the electronic states of the ions-activators and their lattice location, as well as the crystals' luminescent properties at temperatures of 77 and 300 K.

2. Experiment

The crystals were grown from a molten mixture of Li_2CO_3, MoO_3 and ZnO. As lithium zinc molybdate melts with partial decomposition: $Li_2Zn_2(MoO_4)_3 \rightarrow Li_2MoO_4 + 2ZnMoO_4$, a stoichiometric excess of Li_2CO_3 and MoO_3 in the amount of 10–15 mol % was taken to eliminate formation of $ZnMoO_4$.

The optically homogeneous crystals were grown in the conditions of small temperature gradients (~1 degree/cm) by the Czochralski method [22] with seed crystals oriented along directions [100] and [010] from a platinum crucible with 70 mm diameter and 120 mm height. The rate of pulling was ~0.5 mm/h along [100]. For embedding transition metals ions into the crystal structure a certain amount of these metals' oxides was added to the mixture. The electronic state and lattice location of the transition metals ions were investigated by EPR method. EPR spectra were recorded with a Varian EPR spectrometer E-109 equipped with an analog-to-digital data signal converter and proprietary software for storing and processing spectrum data, at temperatures of 77 and 300 K. Optical absorption spectra were recorded with a spectrophotometer in the range 200–800 nm. Luminescence spectra and luminescence lifetimes were recorded with a FLS920 Edin-

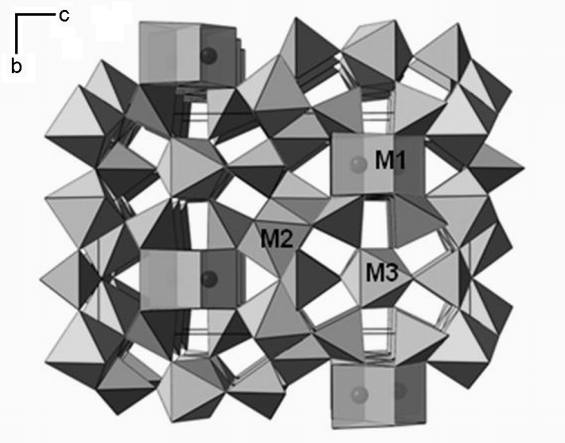

Fig. 1. The structure of $Li_2Zn_2(MoO_4)_3$ crystal.

burg Instrument spectrometer and with a flash photolysis machine in Institute of Chemical Kinetics and Combustion SB RAS.

3. Results and discussion

3.1. Pure $Li_2Zn_2(MoO_4)_3$ crystals

Large (up to 100 mm) optically homogeneous $Li_2Zn_2(MoO_4)_3$ crystals have been grown by the Czochralski method. The X-ray diffraction studies have yielded the following results. Composition: $Li_{2-2x}Zn_{2+x}(MoO_4)_3$ ($0 \le x \le 0.28$) at 600°C. Melting point: 885°C (incongruent). Syngony: rhombic. Structural formula — $Li_{2-2x}Zn_{2+x}(MoO_4)_3$. Space group — *Pnma*, lattice parameters: $a = 5.1100(2)$, $b = 10.5070(6)$, $c = 17.6474(10)$, $Z = 4$, $R = 0.0227$. According to the data obtained, there are three possible zinc ion locations in $Li_2Zn_2(MoO_4)_3$ structure (see Fig. 1). The conducted absorption spectra studies of the pure $Li_2Zn_2(MoO_4)_3$ crystals have shown that the crystals are transparent in the range up to 300 nm. Study of the luminescent properties of $Li_2Zn_2(MoO_4)_3$ crystals has demonstrated that upon band-to-band excitation (300 nm) at room temperature luminescence with $\lambda_{max} = 388$ nm is observed (see Fig.2 curve *1*).

Furthermore, luminescence decay at room temperature reveals a biexponential dependence with $\tau_1 = 2$ ns and $\tau_2 = 6$ ns. Such values of luminescence lifetimes are unique in the range of the known scintillators and exceed requirements for the new scintillators generation.

At 77 K the luminescence spectrum shifts to the long-wave region with $\lambda_{max} = 560$ nm (see Fig. 2 curve *2*). *The luminescence observed at* 77 K is characterized by lifetime $\tau = 100$ ns, which is also a better value in

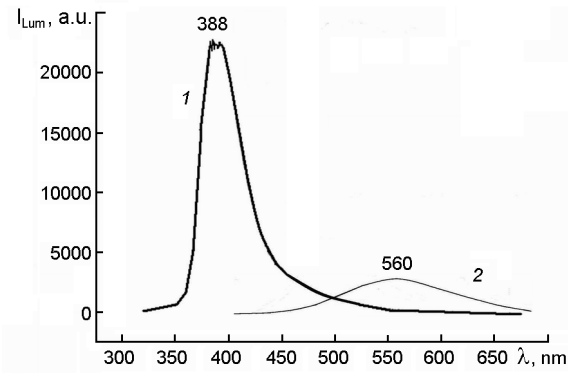

Fig. 2. Luminescence spectra of pure $Li_2Zn_2(MoO_4)_3$ crystal: *1* – at 300 K, *2* – at 77 K.

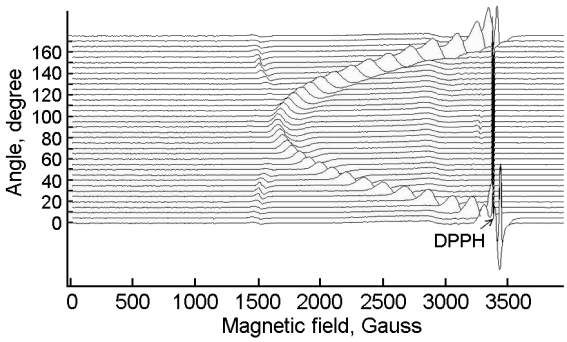

Fig. 3. Angular dependence of Cr^{3+} ions EPR spectrum in $Li_2Zn_2(MoO_4)_3$:Cr crystal.

comparison with the widely used BGO crystals. The data obtained on luminescence of lithium zinc molybdate crystals characterizes them as promising scintillators for high-energy particles.

3.2. $Li_2Zn_2(MoO_4)_3:Cr^{3+}$

In EPR spectra of $Li_2Zn_2(MoO_4)_3$ crystals doped with chrome ions (0.01 and 0.1 mol.%) there is an anisotropic EPR spectrum observed with an effective spin $S_{eff} = 1/2$ and g-factors $g_{\|} = 1.9646$ and $g_{\perp} = 3.9394$ (Fig. 3).

The observed parameters correspond to the case of a strong crystal field ($h\gamma < D$) for the actual spin state of Cr^{3+} ions with $S = 3/2$ and $g_{\|} = 1.9646$ and $g_{\perp} = 1.9696$. Study of the angular dependence has shown that there are two magnetically unequivalent positions in the spectrum. Besides, the angle between them is 7°, which is equivalent to the angular orientation of the prisms in the oxygen surrounding of zinc ions M3. I.e. this data allows us to state that chrome ions occupy zinc M3 location. Possibility for $Li_2Zn_2(MoO_4)_3$ structure to have lithium and zinc ions in the varied

M1–M3 locations enables embedding of trivalent ions into the crystal structure, providing charge compensation by means of replacing zinc with lithium in the adjacent oxygen octahedron. Crystals activated by chrome ions at room temperature and at 77 K exhibited luminescence in the form of a broad line with a maximum at λ_{max} = 560 nm, just like in the case of the pure crystal (see Fig. 2).

3.3. $Li_2Zn_2(MoO_4)_3:Cu^{2+}$

The conducted studies of angular dependence of the EPR spectrum have shown that copper ions replace zinc ions primarily in the one of three possible lattice locations — M2, and these ions have $3d^9$ ground state with electron spin $S = 1/2$. The EPR spectra are characterized by the following spin Hamiltonian parameters: $g_{\|} = 2.38$, $g_{\perp} = 2.06$, $A_{\|} = 116$ G, $A_{\perp} = 0$ G [23]. The vectors of the principle values $g_{\|}$ and $A_{\|}$ coincide and correspond to the oxygen-oxygen direction in the oxygen octahedron of zinc ions M2. And their values are characteristic of the octahedral oxygen surrounding of copper ions.

As was mentioned in the publication [23] increase of copper ions concentration (0.01, 0.03 and 0.05 mol. %) causes growth of 560 nm luminescence intensity. Dependence of the line width on the angle between the direction of the magnetic field vector and the principle values of g and A-tensors constitutes a specific characteristic of the EPR spectra observed. Moreover, such a dependence of line width in the EPR spectra is accompanied by deviation from equidistant line splitting in the hyperfine structure spectrum. At the same time, near the principle values of A and g-tensors line broadening is also accompanied by increase of line splitting (Fig. 4a,b). The studies performed at temperatures of 77 and 300 K have shown that line width and line splitting did not depend on the temperature. Accidental off-orientation of oxygen octahedra containing copper ions due to lattice distortion by other defects could be a possible cause of such peculiarities in the EPR spectra. Judging by the structure of lithium zinc molybdate crystals itself we can state that it originally permits lithium and zinc nonstoichiomentry.

As lithium and zinc ions are differently charged, this in its turn leads to formation of cationic vacancies. Embedding bivalent and higher valence ions of transition metals into the lattice leads to imbalance of lithium and zinc ions ratio, which generates an additional number of cationic vacancies in the localization region of the transition metal ions for charge compensation. On the assumption that cationic vacancies in different lattice locations randomly distort the adjacent oxygen surrounding of copper ions we have conducted a model study of influence of such distortion on EPR spectra. It emerged that in this case the reverse situation occurs near the extreme points of anisotropy of g-factor and hyperfine interaction. Lines in small fields for $g \sim g_{max}$ in the spectra modelled prove to be the most broadened, meanwhile the experimental spectrum gives lines of minimum width in small fields and the shortest distances between transitions (Fig. 4a). In the experimental spectrum for HFS with $g \approx g_{min}$ for quartet transitions in a higher magnetic field both the line width and line splitting decrease (Fig. 4b). However the reverse situation is observed for the spectrum modelled on the assumption of scattering of the vectors directions of the principle values of g and A — tensors. Thus, such model provides no explanation for the peculiarities observed in the EPR spectrum. On the other hand, the presence of a cationic vacancy close to the copper ion as well as varied distance between the vacancy and the oxy-

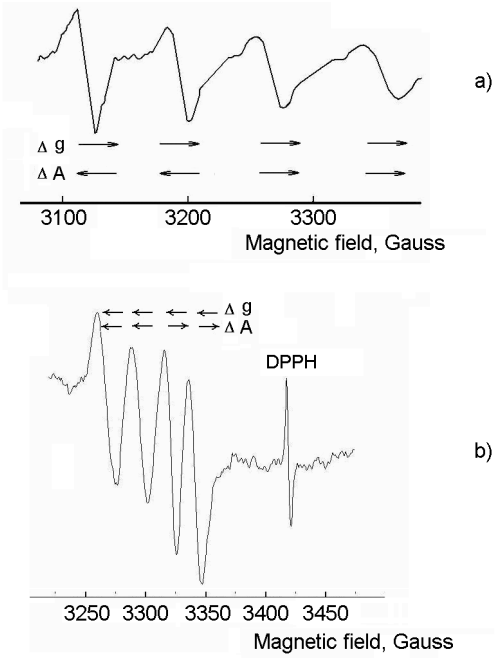

Fig. 4. EPR spectra of Cu^{2+} ions in $Li_2Zn_2(MoO_4)_3$:Cu crystal: a — at $g = 2.38$, b — nearly to $g_{\perp} = 2.06$. The arrows show displacements of EPR lines due to changing of g and A values.

gen octahedron of the copper ion primarily affect the charge distribution in the oxygen octahedron and, as a result, values of *g*-factors and HFS constants.

At the same time, an increase of the HFS constant A_{zz} is virtually always observed along with a decrease of g_{zz}. Such a scatter of the parameters results in transition lines less affected by disturbances in small fields for g_{zz} and remaining narrow. The transition lines (within one HFS quartet) broaden in high fields and the distance between them increases. Moreover, *g*-factor variations cause a shift of all the lines in the quartet of the copper ion hyperfine structure. And a variation (decrease) of the HFS constants leads to a situation when the lines shift depends on the value and sign of the projection of the nuclear magnetic moment. Consequently, this results in a different shift of the transition lines and non-equidistance between them (see Fig. 4a). For the EPR spectrum near g_{xx}, g_{yy} an analogous situation occurs: the transition lines remain narrow in high fields and along with magnetic field decrease the EPR spectrum lines broaden and the distance between them increases (Fig. 4b). This data provides direct evidence that there are cationic vacancies close to the copper ion location. And it is their random distribution in the structure exactly that leads to scatter of the values of *g*-factors and HFS constants.

In order to test scintillation properties of $Li_2Zn_2(MoO_4)_3$ crystals, their cathode-luminescence has been studied. The studies performed have revealed that cathode-luminescence is also observed with the maximum at 560 nm. And intensity of cathode-luminescence of a copper-doped $Li_2Zn_2(MoO_4)_3$ sample as well as of luminescence in the range of 560 nm grows along with temperature decrease. Such a dependence of the photoluminescence and cathode-luminescence intensity on the copper ion concentration gave us grounds to suggest that the copper ions are responsible for the low-temperature luminescence with $\lambda_{max} = 560$ nm [23]. However, as further studies of both pure crystals and crystals doped with other transition metal ions demonstrated, the luminescence with $\lambda_{max} = 560$ nm is not primarily connected with embedding of copper ions into the structure of $Li_2Zn_2(MoO_4)_3$ crystals.

3.4. $Li_2Zn_2(MoO_4)_3:Fe^{3+}$

Incorporating 0.01 mol. % of iron ions into the structure of $Li_2Zn_2(MoO_4)_3$ crystals imparted a grey colour to the crystals and significantly deteriorated transmission spectra in the visible wavelength range. Moreover, an intensive absorption band appeared in the range of 500 nm in optical spectra. Crystals activated by iron ions also demonstrated luminescent properties. Unlike with copper ions, here maximum luminescence was observed at 520 nm. Study of the EPR spectra in the range 9.5 and 35 GHz has shown that iron ions occupy lattice location M2 in $Li_2Zn_2(MoO_4)_3$ crystal with the charge state Fe^{3+}. Analysis of the angular dependence of EPR spectra using the program [24] allowed us to calculate the fine structure parameters for Fe^{3+}, which respectively equal the following values: $S = 5/2$, $g = 2.00$, $D = 1800$ G and $E = 16$ G. EPR spectra of iron ions in lithium zinc molybdate crystals are characterized by variation of the line width depending on the crystal orientation from 200 to 500 G. But at the same time, the line width does not depend on the temperature, just like in the case with copper ions. The effects observed in the copper EPR spectra give an insight into the factors causing such broad lines in the iron EPR spectra. The dependence of charge distribution on the distance from a cationic vacancy determines the scatter of the crystalline field parameters *D* and *E*. This leads to the situation when for the angle $\varphi = 54°$ $\sum D_i(3\cos^2\varphi - 1)$ goes to zero and the EPR spectrum line width equals 200 G. And as the angle deviates from 54° the set of parameters D_i leads to a visible broadening of the EPR spectrum lines.

3.5. $Li_2Zn_2(MoO_4)_3:Ti^{4+}$

$Li_2Zn_2(MoO_4)_3$ crystals doped with Ti^{4+}, just like pure crystals, were grown in the conditions of small temperature gradients (~1 degree/cm) from a molten mixture with a stoichiometric excess of Li_2CO_3 and MoO_3 in the amount of 10–15 mol %, with seed crystals oriented along [010]. For the doping TiO_2 was added to the mixture. The growth rate of the homogeneous crystals doped with titanium in the amount up to several percent was found to be virtually the same as that of the pure crystals: ~0.5 mm/h, which appears to be determined by isostructurality of $Li_2Zn_2(MoO_4)_3$ and $Li_3Ti_{0.75}(MoO_4)_3$ crystals (Fig. 5).

In the absorption spectra of $Li_2Zn_2(MoO_4)_3$ crystals activated by 0.02 and 0.2 mol. % of titanium additional lines did not appear in the visible region. No tita-

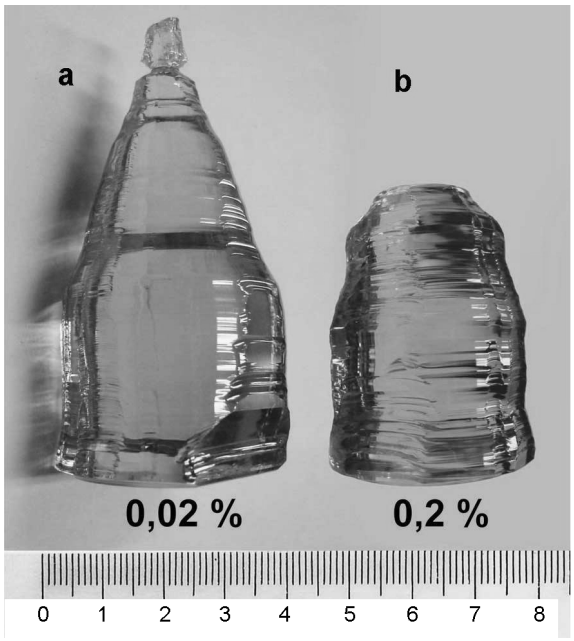

Fig. 5. As-grown $Li_2Zn_2(MoO_4)_3$ crystals, doped by Ti^{4+} ions.

nium spectra are observed in the EPR spectra of the crystals. This means that titanium is diamagnetic and is embedded in $Li_2Zn_2(MoO_4)_3$ structure in the state Ti^{4+}. Owing to absence of EPR spectra it's difficult to speak about the lattice location of the titanium ions. Probably they occupy the molybdenum location. In this case however the luminescence intensity with $\lambda = 560$ nm has to decrease along with growth of titanium concentration, because an excessive amount of bivalent zinc is required in lithium locations for charge compensation. Experimentally the reverse dependence is observed, i.e. along with growth of titanium concentration in the growing medium the luminescence intensity with $\lambda = 560$ nm increases. At the same time titanium-doped crystals grow well only with an excess of lithium ions in the growing system, which substantiates our assumption that titanium ions occupy zinc locations. The studies of luminescent properties of $Li_2Zn_2(MoO_4)_3$ crystals activated by titanium ions reveal a more intensive luminescence with $\lambda = 560$ nm in comparison with crystals activated by other ions. This gives us grounds to assume that, like in the case of other transition metals ions, titanium ions primarily occupy zinc location generating additional cationic vacancies. In Fig. 6 luminescence spectra of $Li_2Zn_2(MoO_4)_3$ crystals are shown for different titanium concentrations at room temperature and 77 K. The same as in the case

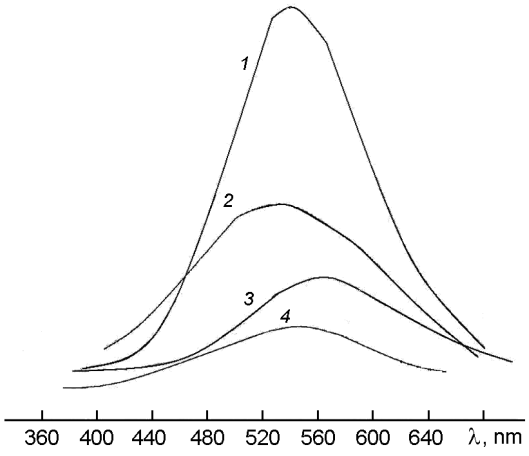

Fig. 6. Luminescence spectra of $Li_2Zn_2(MoO_4)_3$÷Ti crystals: *1* — doped by 0.2 % Ti, $T = 77$ K; *2* — doped by 0.2 % Ti, $T = 300$ K; *3* — 0.02 % Ti, $T = 77$ K; *4* — 0.02 % Ti, $T = 300$ K.

of other transition metals ions, here the luminescence intensity with $\lambda = 560$ nm increases along with temperature decrease.

4. Conclusions

Large crystals, both pure and doped with different transition metal ions — Cu, Fe, Cr, Ti, have been grown by the low-gradient Czochralski method. The conducted studies of $Li_2Zn_2(MoO_4)_3$ allowed us to determine the charge state and lattice location for Cu, Fe, Cr ions. It has been found that luminescence with very short lifetimes is observed in pure $Li_2Zn_2(MoO_4)_3$ crystals, that allows us to speak about the crystals as a promising scintillation material. It has been determined that low-temperature luminescence with $\lambda_{max} = 560$ nm depends on both the nature of transition metals ions and their concentration. It is assumed that low-temperature luminescence is defined by cationic vacancies providing charge compensation of transition metals ions.

References

1. M.Globus, B.Grinyov, K.K.Jong, Inorganic Scintillators for Modern and Traditional Applications, Institute for Single Crystals, Kharkiv, Ukraine (2005).
2. M.Kobayashi, M.Ishii, C.L.Melcher, *Nucl. Instr. and Meth. Phys. Res.* **A335**, 509 (1993).
3. C.L.Melcher, J.S.Schweitzer, *IEEE Trans. Nucl. Sci.*, **NS39**, 502 (1992).
4. C.Dujardin, C.Pedrini, D.Boutet, J.W.M.Verweij et al., in: Proc. of the Intern. Conf. "SCINT 95", ed. by P.Dorenbos, C.W.E.van Eijk, Delft, the Netherlands (1995), p.36.

5. C.W.E.van Eijk, *Nucl. Instr. and Meth. Phys. Res.*, **A392**, 285 (1997).
6. D.Pauwels, N.Lemasson, B.Viana et al., Inorganic Scintillators and Their Applications, in: Proc. of Intern. Conf."Scint. 99", ed. by V.Mikhailin, Moscow, Russia (1999), p.511.
7. F.T.Avignone III, G.S.King III, Yu.G.Zdesenko, *New J. Phys.*, **7**, 1 (2005).
8. G.Audi, A.H.Wapstra, C.Thibault, *Nucl. Phys.*, **A729**, 337 (2003).
9. E.V.D.Van Loef, P.Dorenbos, C.van Eijk et al., *Appl. Phys. Lett.*, **79**, 1573 (2001).
10. M.Kapusta, M.Balcerzyk, M.Moszynski, J.Pawelke, *Nucl. Instr. and Meth. Phys. Res.*, **A42**, 610 (1999).
11. M.Kobayashi, M.Ishii, K.Harada et al., *Nucl. Instr. and Meth. Phys. Res.*, **A373**, 333 (1996).
12. J.B.Reed, B.S.Hopkins, L.F.Audrieth et al., *Inorg. Synth.*, **1**, 28 (1936).
13. K.S.Shah, J.Glodo, M.Klugerman et al., *Nucl. Instr. and Meth. Phys. Res.*, **A505**, 76 (2003).
14. R.Zhu, in: Proc. of the Intern. Conf. "SCIN 97", ed. by Zhiwen et al., Shanghai, China (1997), p.73.
15. V.B.Mikhailik, H.Kraus, D.Wahl, M.S.Mykhaylyk, *Phys. Stat. Sol. B*, **242**, 17 (2005).
16. Yu.G.Zdesenko, B.N.Kropivyanskii, V.N.Kuts et al., *Instr. Exp. Tech.*, **39**, 362 (1996).
17. L.Xue, Y.Wang, P.Lv, D.Chen et al., *Cryst. Growth Design.*, **9**, 914 (2009).
18. L.Xue, Z.Lin, F.Huang, J.Liang, *Chin J. Struct. Chem.*, **26**, 1208 (2007).
19. V.A.Efremov, V.K.Trunov, *J. Inorgan. Chem.*, **20**, 2200 (1975).
20. V.A.Efremov, Yu.G.Petrosyan, V.M.Zhukovsky, *J. Inorgan. Chem.*, **22**, 175 (1977).
21. S.F.Solodovnikov, Z.A.Solodovnikova, E.S.Zolotova et al., *J. Solid State Chem.*, **182**, 1935 (2009).
22. A.A.Pavlyuk, Ya.V.Vasiliev, L.Yu.Kharchenko, F.A.Kuznetsov, in Proc. of the Asia Pacific Society for Advanced Materials APSAM-92, Shanghai (1992), p.164.
23. V.A.Nadolinny, N.V.Cherney, A.V.Sinicin et al., *J. Struct. Chem.*, **49**, 891 (2008).
24. N.V.Cherney, V.A.Nadolinny, *Zavodskaya Laboratoriya*, **72**, 20 (2006).

Вплив домішкових іонів перехідних металів на люмінесцентні властивості кристалів $Li_2Zn_2(MoO_4)_3$

В.А.Надолинный, А.А.Павлюк, А.А.Рядун, А.А.Трифонов, С.Ф Солодовников, З.А. Солодовникова, О.С. Золотова, В.Ф. Плюснин, М.І.Рахманова, Є.Г.Богуславський

На основі откорегованої фазової діаграми вибрано правильні умови росту кристалів $Li_2Zn_2(MoO_4)_3$ і вирощено великі кристали (до 100 мм) як бездомішкові, так і активовані іонами перехідних металів - Cu, Cr, Fe, Ti. Методом ЕПР встановлено зарядовий стан і структурне положення іонів перехідних металів. Проведені дослідження люмінесцентних властивостей показали, що для бездомішкових кристалів при кімнатній температурі спостерігається люмінесценція з λ = 388 нм з двоекспоненціальним спадом люмінесценції з τ_1 = 2 нсек и τ_2 = 6 нсек. При 77 К як для бездомішкових, так і для активованих іонами перехідних металів кристалів спостерігається люмінесценція з λ= 560 нм і часом життя люмінесценції τ = 100 нсек, причому інтенсивність люмінесценції з λ= 560 нм залежить від природи і концентрації іонів перехідних металів. Припускається, що за низькотемпературну люмінесценцію відповідають катіонні вакансії, відповідальні за зарядову компенсацію домішкових іонів перехідних металів.